LEGIBILITY NOTICE

A major purpose of the Technical Information Center is to provide the broadest dissemination possible of information contained in DOE's Research and Development Reports to business, industry, the academic community, and federal, state and local governments.

Although a small portion of this report is not reproducible, it is being made available to expedite the availability of information on the research discussed herein.

LA-UR
CONF-891017--2

Received by OSTI
JUN 07 1989

Los Alamos National Laboratory is operated by the University of California for the United States Department of Energy under contract W-7405-ENG-36

LA-UR--89-1713
DE89 013441

TITLE LABORATORY CROSS-BOREHOLE IMAGING OF UNCONSOLIDATED SEDIMENTS

AUTHOR(S) P.A. Johnson, ESS-4
T.H. Larkin, MEE-13
W.S. Phillips, ESS-4
G. Eischeid, ESS-4

SUBMITTED TO SEG Annual Fall Meeting

Los Alamos Los Alamos National Laboratory
Los Alamos, New Mexico 87545

LABORATORY CROSS-BOREHOLE IMAGING OF UNCONSOLIDATED SEDIMENTS

Paul A. Johnson, Timothy H. Larkin,
W. Scott Phillips*, and Greg Eischied

Earth and Space Sciences Division, Los Alamos National Laboratory, Los Alamos, New Mexico
(* consultant)

SUMMARY

Cross-borehole elastic wave tomography offers great potential for subsurface imaging of sediments and associated fluids. Using this method we created a high resolution tomographic image of velocity structure obtained from laboratory generated compressional wave traveltimes in unconsolidated sediments. The image shows three layers and a water filled container located in the center of the middle layer. An image obtained from computer simulated traveltimes shows good agreement with the image from laboratory data. Source frequency was 135 kHz, velocities ranged from 1.4 to 1.8 km/s, and thus wavelengths were 1.0 to 1.4 cm. Distance between boreholes was 30 cm with about 60 cm of vertical coverage. Over 900 raypaths were used in the image. The seismic quality factor Q ranged from 11 to 25 in the two saturated sediments.

Our immediate application of this method is to ecological problems. However, such a method could be applied to small scale hydrological problems and other areas of interest where fluid content is of interest.

INTRODUCTION

Understanding subsurface geological and hydrological processes is limited by the lack of non-invasive field tools. Currently used methods for detailed field study of sediments and fluids often involve destructive sampling by drilling extensively or excavation. Several geophysical tools may enable remote, non-invasive characterization of these media. These include gravity, magnetic, electromagnetic, and elastic wave techniques. Each technique measures different physical properties. In this study we use high frequency elastic waves to characterize velocity-density variations (acoustic impedance contrasts).

Our effort has been devoted to laboratory development and testing of cross-borehole elastic wave tomography. Our goal is to develop a tool that can be used for high resolution, small scale, in situ imaging of sediments. A tool of this type could be emplaced for long periods of time to monitor such things as temporal variations in fluid content. In this study, we image layers composed of quartzo-feldspathic sands and clay-rich quartz sands to test the possibility of using the method in unconsolidated, water saturated media. By imaging less energy absorptive materials such as sands, we are a step closer to working with media that are more attenuating to elastic wave energy such as clays, soils, and undersaturated materials.

This paper describes an imaging experiment in layered sediments, with an embedded low velocity zone. We evaluate the imaging results by comparing them to results obtained using computer simulated traveltimes.

SOURCE/RECEIVER DESIGN

Constructing sources and receivers that operate effectively in sediments is difficult because, among other problems, much of the excited energy normally goes into exciting tube waves rather than body waves. We found the following design effective at coupling body waves into, and out of, the medium. Cylindrical piezoelectric transducers (PZTs) were used for both sources and receivers. The diameters of the source and receiver PZTs are 2.54 cm and 1.06 cm, respectively. Each PZT was placed inside a Teflon (a registered trademark of Dupont Corporation) container filled with silicon oil. Container tests with a variety of materials showed that Teflon had a good impedance match with the sediments, and therefore the best transmission and reception properties. The Teflon container was threaded at both ends so that each container could be attached to other, identical containers.

We stacked eight PZTs to form source and receiver stringers. Thus signals from 64 raypaths could be collected without moving either stringer, minimizing disruption of the sediments. Movement of the stringers was controlled by hand using plexiglas pipes fitted to both ends of the stringers and supported by guides at the container top and bottom. The guides allowed us to measure vertical distance changes precisely and to minimize horizontal distance uncertainties by restricting lateral movement.

In our past experiments using other source designs, much of the source energy produced tube waves trapped within the source borehole instead of compressional waves that propagate between sources and receivers. No tube waves were observed once we began using this design.

Each PZT case was wired so that PZTs could be excited independently. The source stringer was wrapped in aluminum foil to inhibit transmission of EM noise. Both source and receiver stringers were then encased in heat-shrink tubing to protect wiring and foil from abrasion during stringer movement.

EXPERIMENTAL CONFIGURATION

Figure 1 shows a block diagram of the experimental configuration. A Hewlett-Packard 9920 function generator supplied a tone burst amplified by a Krohn-Hite power amplifier. The signal was transmitted by one of the PZTs in the source stringer, detected at a single receiver, and relayed through a preamplifier to a LeCroy 9400 digital oscilloscope. Compressional wave traveltimes were read on the waveform recorder using cursors at high vertical gain, and signals were then sent to an HP 9816 computer for storage and plotting. An algorithm developed for the computer controlled the imaging experiment and all associated apparatus.

TOMOGRAPHY EXPERIMENT

The tomography experiment was conducted inside a plastic barrel measuring approximately 90 cm high by 61 cm wide as shown schematically in Figure 2. We used two sediments in the tomography experiment. The first was a concrete-grade, quartzo-feldspathic sand containing 5% other minerals, mostly biotite (hereafter termed "concrete sand") with grain sizes in the order of 0.5 to 2 mm. The second material was a clay rich, silty-sand with grain sizes of 0.1 to 1 mm, obtained from the banks of the Rio Grande (hereafter termed "RG sand").

The area imaged was composed of three layers as shown in Figure 2: the RG sand was used for the top and bottom layers, and the concrete sand was used for the middle layer. All layers were 100% water saturated. Water was added through a valve from the container bottom; adding water from below forced air to the surface. Gravel was used as the lowermost layer in the container to evenly distribute water at the base. Once all layers were saturated, the water was cycled out of and back into the layers several times. In this manner we were able to compact the sediments more quickly and force out virtually all air.

A 10 x 10 x 10 cm water filled container was buried in the center of the middle layer. The container was made of supple plastic with walls 0.02 cm thick. The water container was used to see if we could distinguish between saturated sand and a water filled container. A 17 cm layer of concrete sand was placed above the uppermost layer to add lithostatic pressure, compacting the layers and thereby enhancing elastic wave coupling. Plastic film several micrometers thick was placed between each layer to inhibit sediment mixing and thereby produce sharp boundaries. The plastic fiim was perforated so that water passage was not blocked.

The region to be imaged was located in the center of the container to avoid side-wall reflections arrived well behind the first arriving compressional wave that would not interfere with traveltime interpretations (Figure 2). Once the layers were in place and water cycling was complete, the set-up was left standing for several days for further consolidation so that little or no change would take place during the experiment.

DATA COLLECTION

A single pulse of 135 kHz and 80 Volts was used to excite the source at a repetition rate of 10 milliseconds. Received signals were summation averaged a minimum of 100 times and up to a maximum of several thousand times depending on the signal-to-noise ratio. Traveltimes were visually determined from the expanded scales available on the waveform recorder.

Data collection took place as follows. A source was excited for each receiver. Then, the next source was excited for all receivers, and so on, until 64 signals were collected from all possible combinations of sources and receivers. After these 64 signals had been collected, the source stringer was moved downward, 64 more signals were collected. The receiver stringer was then moved downward and again the collection procedure was repeated. In this manner we collected 960 signals through the layered region. The angle between source and receivers ranged from +- 59 degrees, as measured from horizontal.

TOMOGRAPHY ALGORITHM

The computational method we used for obtaining a velocity tomograph from observed compressional wave traveltimes is known as iterative backprojection. The minimum energy technique we use is described by Dines and Lytle (1979). Using this method, we found simultaneous iterative reconstruction SIRT to produce better images than algebraic reconstruction, ART.

To simplify the calculations we assumed straight raypaths. This is equivalent to assuming that only small fluctuations exist in material to be imaged, such that refraction effects can be ignored. Dines and Lytle (1979) were able to apply straight ray techniques successfully in cases where the velocity fluctuation was 16%. We expect 20% velocity variation based on our preliminary experiments. Therefore, the velocities are such that adding bending rays may improve inversion results.

Our method also includes an optional two-dimensional smoothing algorithm of arbitrary size and shape that operates between the backprojection iterations and helps to remove any model oscillations of such small scale to be deemed unrealistic.

To establish the quality of the tomographic reconstruction from observed traveltimes, a computer generated tomograph was created using model data for comparison with the real data result. Computer generated raypaths and corresponding traveltimes were obtained using a model of the imaged region. These data were then inverted to create a tomograph of "perfect data".

RESULTS

Signals were collected for 960 raypaths through the region of study. Over 64 raypaths were observed again after the completion of the experiment to test whether or not further compaction had affected the observations over the duration of the experiment. Note that increasing the rate of data collection is a simple matter. Using a recorder with many data collection channels and a computer algorithm for automatic traveltime determinations could allow an experiment to be conducted in tens of minutes.

The observed traveltimes matched the original measurements within the accuracy. Traveltime observation error (accuracy) was less than 2.0 microseconds (1.2 % of total traveltime), and estimated precision was 1.0 microsecond (0.6 %). The accuracy was estimated from the traveltime measurement error due to the uncertainty in determining the arrival time for emergent signals. The estimate of precision was determined from repeated observations of a single traveltime.

The imaged velocity cross-section obtained is shown in Figure 3a. The outline in white illustrates the location of boundaries between layers and the location of the water container. We discarded traveltimes that were unrealistically large at each iteration step because large traveltimes are more likely to be poorly determined. Figure 3b shows traveltime inversion results from perfect data with noise added. In the case of perfect data with noise, gaussian noise with a standard deviation of 1.0 microsecond (our estimated precision) was added to more realistically simulate real data. A 50 by 50 matrix of pixels was used in the inversions, and the images shown were produced with 12 iterations. Darker tones represent faster velocities and lighter tones represent slower velocities. The calculated velocity range of the concrete sand is between 1.75 and 1.85 km/s; for the RG sand the range is 1.60 - 1.75; and for the water the range is 1.65 - 1.70 km/s. All of these velocities are faster than actual measured velocities for individual materials. Table 1 shows the measured average velocities of individual materials at full saturation, and Q-values, obtained from previous experiments, for each material.

Smoothing was performed between iterations by averaging adjacent pixel slownesses together. Horizontally adjacent pixels received more weight in the average since resolution is worst in this direction, given the experimental geometry. Smoothing removes unrealistic pixel-to-pixel velocity oscillations that commonly occur, and adds redundancy to a problem that would otherwise be underdetermined (fewer data than unknowns).

DISCUSSION

In comparing the tomograph with the actual properties of the imaged region one sees the lower boundary of the concrete sand is reasonably well defined; the upper boundary is more irregular due to poorer traveltime determinations in this region and to inversion artifacts (the "x"-shaped feature emanating from the water container). The low velocity zone corresponding to the water container is well imaged. The container appears as the light region in the center of the image; the top and bottom of the container are clear, however, the sides are smeared horizontally due to the constraint of limited aperture (Aki and Richards, 1980).

The tomographic reconstruction of perfect data with added noise shown in Figure 3b demonstrates that most of the features seen in the laboratory data tomograph appear. This comparison shows that the laboratory imaging was successful. The major difference between the theoretical and observed result is the lack of clear boundaries between layers. The artifact emanating from the water container also exists in the perfect data inversion. It is, however, very weak.

The geometry used to collect our data is responsible for the resolution of and artifacts within the image we obtained. The traveltime data consisted of ray paths propagating at angles +-59 degrees from horizontal; no vertical paths were included. With such a measurement geometry horizontal boundaries will be imaged distinctly, while vertical boundaries will not. The addition of near-vertical ray paths would reduce the non-uniqueness inherent in tomographic reconstructions, and thus features such as the streaking around the water container. This could be accomplished by placing sources or receivers along the surface between the boreholes.

SUMMARY AND CONCLUSIONS

We imaged saturated sediments composed of three-layers and a low velocity volume centered within the middle layer. The low velocity volume was created using a water-filled container. The experiment was conducted in the laboratory using stringers of source and receiver piezoelectric transducers spaced 30 cm apart. The stringers are novel in that they are extremely efficient at coupling compressional waves into the sediment while avoiding tube wave generation. The frequency of operation was 135 kHz and wavelengths were approximately 1 cm in the sediments, with quality factors Q ranging from 11 to 25. Comparison of the tomograph from observed traveltimes and a tomograph generated from theoretical data shows that we succeeded in imaging the sediments. To our knowledge, this is the first time unconsolidated sediments have been imaged at such high resolution using elastic waves under laboratory conditions. This initial imaging experiment under laboratory conditions suggests cross-borehole elastic wave tomography could be developed as a field tool for subsurface imaging of sediments.

ACKNOWLEDGMENTS

We are grateful to Tom Hakonson, Susan Meadows and Paul Rich for helpful discussions. We thank Evon Stepani for help with source and receiver design. This work was conducted under the auspices of the Department of Energy's National Environmental Research Park Program under contract W-7405-ENG-36 with Los Alamos National Laboratory.

Table 1. Media Properties at Complete Saturation

Material	Average Velocity (km/s)	Q
Concrete sand	1.80	25
Rio Grande sand	1.44	11
Water	1.50	

REFERENCES

Aki, K. and P. G. Richards, Quantitative Seismology, 1980, W. H. Freeman and Company, San Francisco.

Dines, K. A. and R.J. Lytle, Computerized geophysical tomography, Proc. IEEE, V. 67, 1065-1073, 1979.

FIGURE CAPTIONS

Figure 1. Block diagram of experimental configuration.

Figure 2. Geometrical relationships within test container.

Figure 3. a) Velocity tomograph from laboratory data showing velocity structure of the region depicted in the overlay. b) Velocity tomograph from computer generated data with added noise. Velocities in km/s shown on tone bar at right.

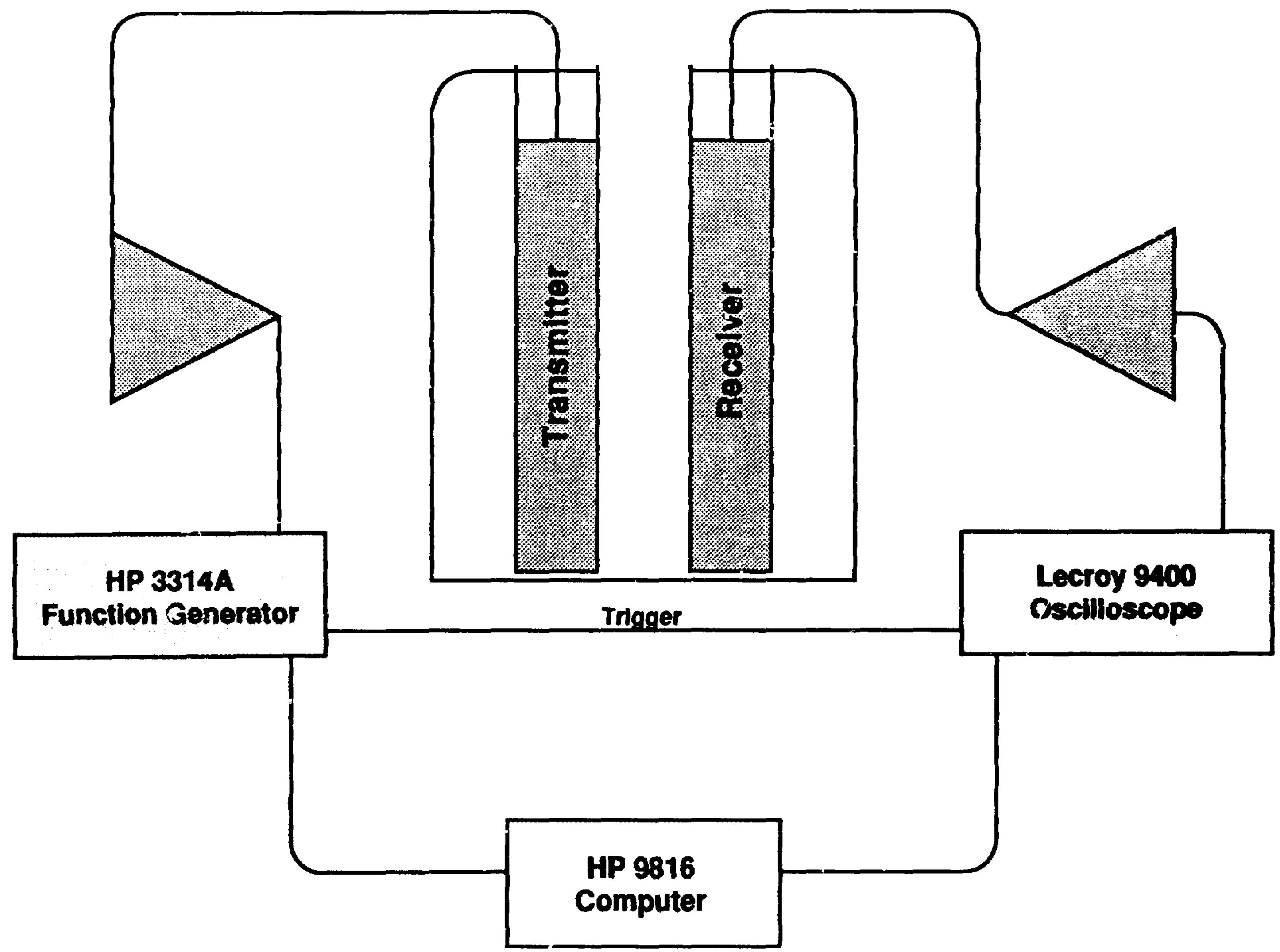
Transmitter
Receiver
HP 3314A
Function Generator
Trigger
Lecroy 9400
Oscilloscope
HP 9816
Computer

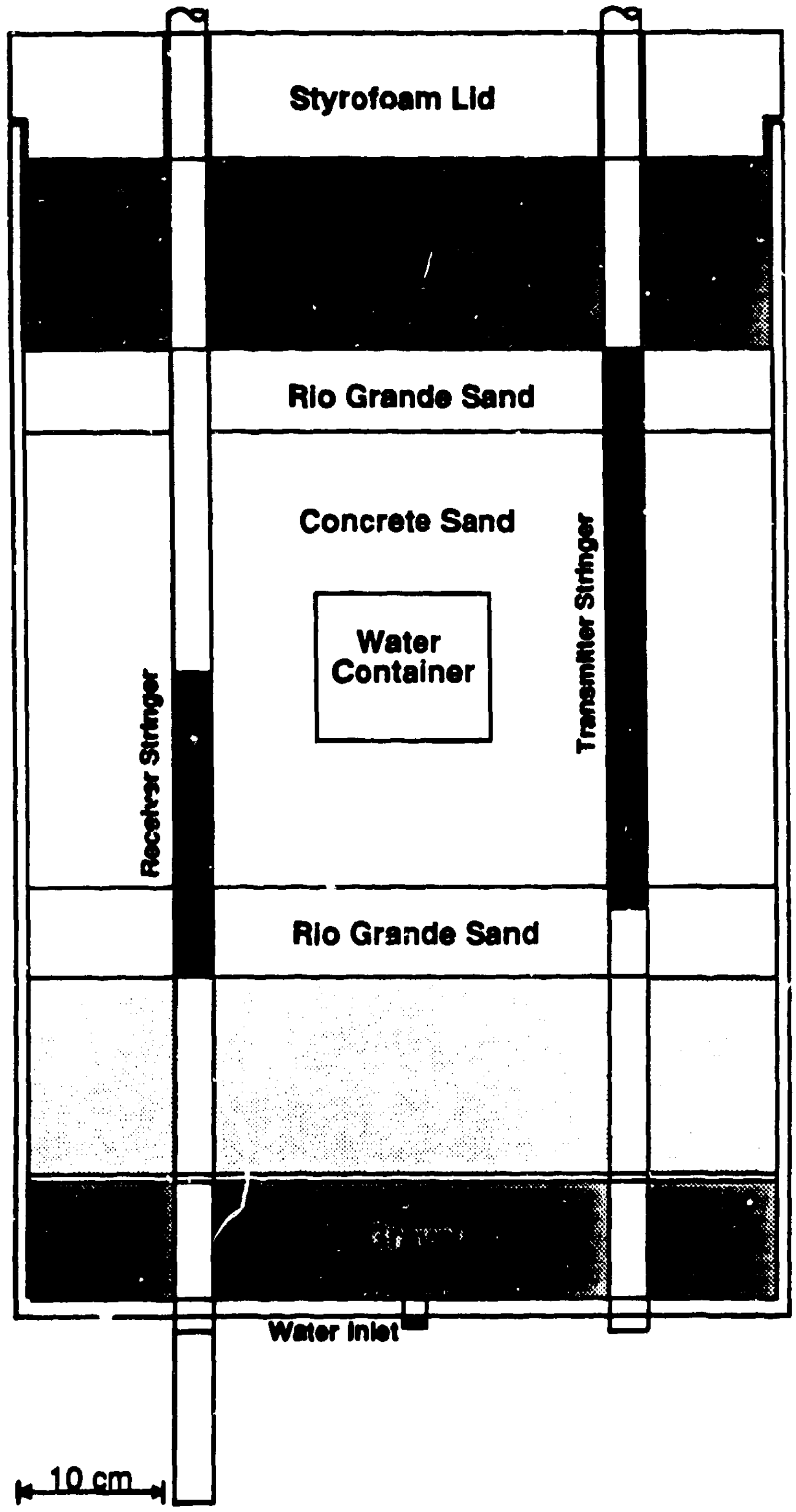

Styrofoam Lid
Rio Grande Sand
Concrete Sand
Water Container
Receiver Stringer
Transmitter Stringer
Rio Grande Sand
Water inlet
10 cm

VELOCITY TOMOGRAPH
LAB DATA

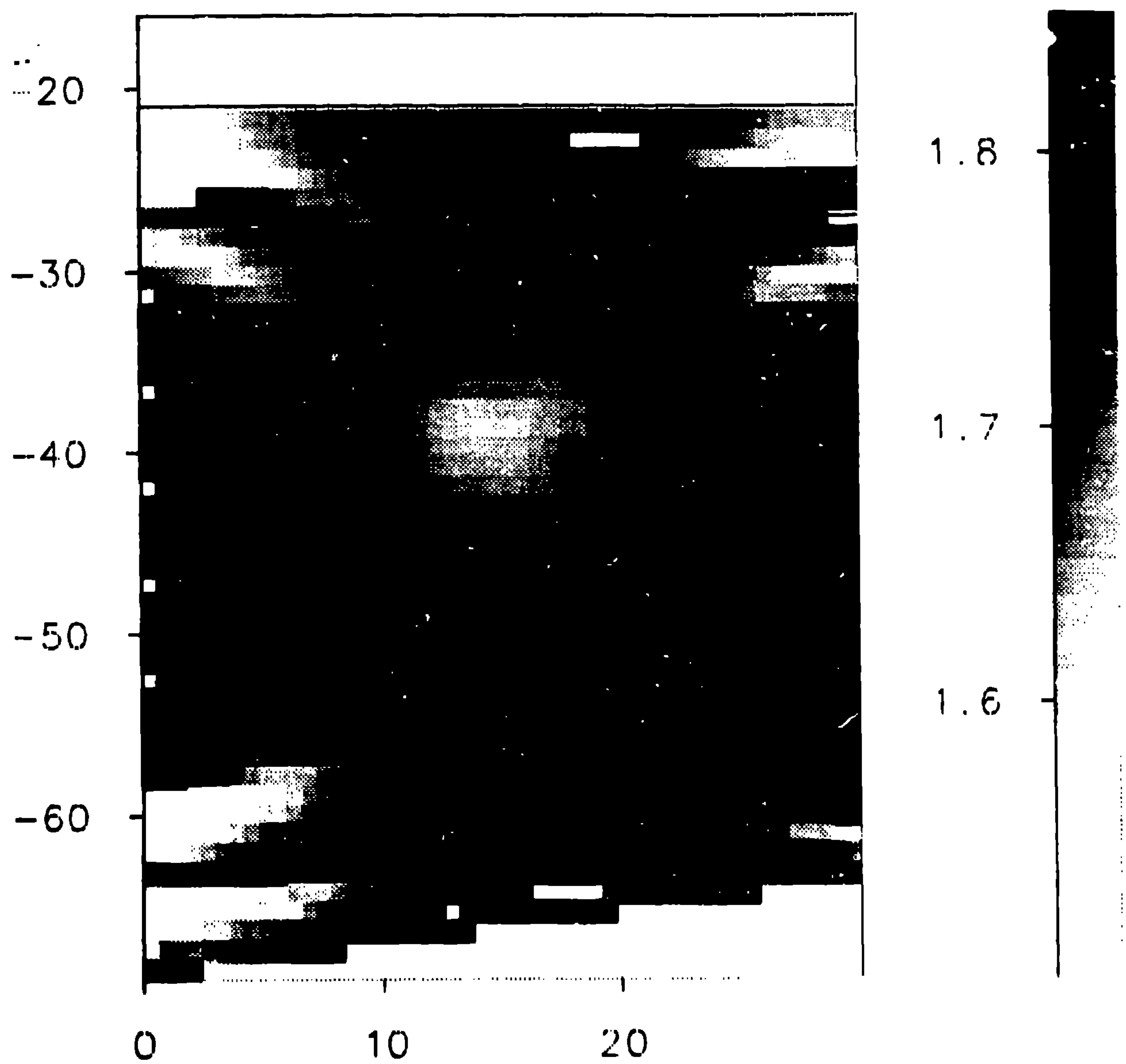

VELOCITY TOMOGRAPH
PERFECT DATA WITH NOISE

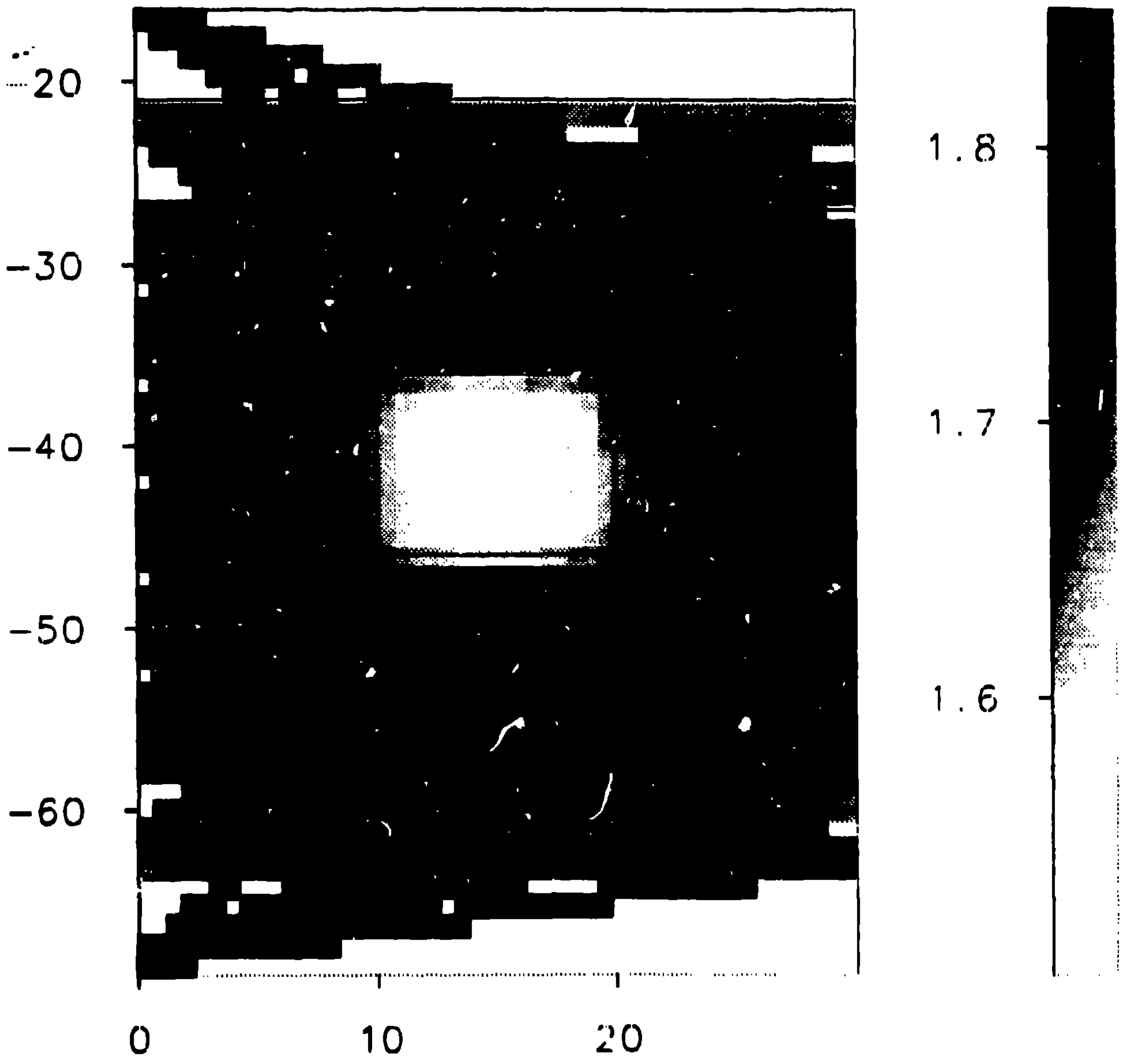

3b